(22) P. Love, R. B. Cohen, and R. W. Taft, *J. Am. Chem. Soc.*, **90**, 2455 (1968).
(23) Ionization potentials for several of the amines listed in Table I have also been reported by D. H. Aue, H. M. Webb, and M. T. Bowers, *J. Am. Chem. Soc.*, **98**, 311 (1976). Although vertical ionization potentials are generally in good agreement, the adiabatic values chosen in the present work are 0.1 eV higher. The most notable discrepancy is in the reported value of the adiabatic ionization potential of Et_3N, which in the present work is 0.31 eV (7.2 kcal/mol) higher than reported earlier. Repeated measurements of the spectrum lead us to believe that the value of 7.42 eV reported in Table I is more reasonable.
(24) W. R. Harshbarger, *J. Chem. Phys.*, **56**, 177 (1972). See also, D. H. Aue, H. M. Webb, and M. T. Bowers, *J. Am. Chem. Soc.*, **97**, 4136 (1975).
(25) T. H. Morton and J. L. Beauchamp, *J. Am. Chem. Soc.*, **94**, 3671 (1972).
(26) PA[CH_3NH_2] = 211.3 kcal/mol, PA[$CH_3(CH_2)_2NH_2$] = 215.5 kcal/mol, and PA[$CH_3(CH_2)_3NH_2$] = 216.0 kcal/mol from ref 11.
(27) J. O. Hirschfelder, C. F. Curtiss, and R. B. Bird, "Molecular Theory of Gases and Liquids", Wiley, New York, N.Y., 1954, p 941f; J. A. Beran and L. Kevan, *J. Phys. Chem.*, **73**, 3860 (1969).
(28) Intramolecular N-H···F hydrogen bonding in 2-fluoroethylamine is discussed by L. Radom, W. A. Latham, W. J. Hehre, and J. A. Pople, *J. Am. Chem. Soc.*, **95**, 693 (1973), and is shown to have an important influence on the stability of different molecular conformations. Related studies of intramolecularly hydrogen-bonded systems using photoelectron spectroscopy include R. S. Brown, *Can. J. Chem.*, **54**, 642 (1976); **54**, 1929 (1976); and S. Leavell, J. Steechen, and J. L. Franklin, *J. Chem. Phys.*, **59**, 4343 (1973).

Molecular Orbital Studies of Electron Donor–Acceptor Complexes. 4. Energy Decomposition Analysis for Halogen Complexes: H_3N–F_2, H_3N–Cl_2, H_3N–ClF, CH_3H_2N–ClF, H_2CO–F_2, HF–ClF, and F_2–F_2

Hideaki Umeyama, Keiji Morokuma,* and Shinichi Yamabe

Contribution from the Department of Chemistry, University of Rochester, Rochester, New York 14627. *Received June 1, 1976*

Abstract: The energy and charge distribution decomposition analyses are carried out for a series of electron donor–acceptor complexes of halogens. Based on the energy components essential for binding, the complexes are qualitatively classified as follows: H_3N–F_2 H_3N–Cl_2, and H_2CO–F_2, weak electrostatic charge transfer complexes; H_3N–ClF, intermediate electrostatic complex; HF–ClF, weak electrostatic complex; and F_2–F_2, very weak dispersion-charge transfer complex. The energy components determining the equilibrium geometry as well as the *N*-methyl substituent effect are also identified, and comparisons between various complexes have been made. The predicted geometry of an anti-hydrogen bonded complex FCl–FH is in good agreement with experiment, but the hydrogen bonded counterpart ClF–HF appears to be comparable in energy. The SCF interaction energy for $(F_2)_2$ favors an open L shape.

I. Introduction

The origin of attractive intermolecular interactions and the factors determining the geometry of molecular complexes have been sought after for decades using numerous experimental and theoretical techniques.[1,2] For hydrogen bonding, which in earlier days had been considered to be a purely electrostatic interaction, the importance of the charge transfer interaction has long been emphasized.[1] The electron donor–acceptor (EDA) complex or the charge transfer complex was originally thought to be stabilized principally by the charge transfer interaction between the donor and acceptor molecules.[2,3] Later studies have suggested that many such complexes, especially weak complexes, are bound primarily due to the electrostatic and polarization interactions.[4,5] Since the interaction is quantum mechanical in nature, quantum chemical calculations should be able to provide substantial information regarding the nature of the binding.

The ab initio SCF molecular orbital (MO) method has been very successful in both predicting the equilibrium geometry and stabilization energy of many hydrogen bonded and EDA complexes and in interpreting the nature of such interactions.[6,1b] The energy and charge distribution decomposition (ECDD) analyses proposed by Morokuma[7] and Kitaura and Morokuma[8] have provided a means for direct examination of the origin of molecular interactions.[9-15] Using either the model wave function or model Hartree–Fock operator they unambiguously defined components of the total interaction, ΔE_{SCF}, which are in accord with traditional viewpoints.[16]

$$\Delta E_{SCF} = ES + PL + EX + CT + MIX \qquad (1)$$

The individual components have the following physical significance.[17]

ES is the electrostatic interaction, i.e., the interaction between the undistorted electron distribution of a monomer A and that of a monomer B. This contribution includes the interactions of all permanent charges and multipoles, such as dipole–dipole, dipole–quadrupole, etc. This interaction may be either attractive or repulsive.

PL is the polarization interaction, i.e., the effect of the distortion (polarization) of the electron distribution of A by B, the distortion of B by A, and the higher order coupling resulting from such distortions. This component includes the interactions between all permanent charges or multipoles and induced multipoles, such as dipole–induced dipole, quadrupole–induced dipole, etc. This is always an attractive interaction.

EX is the exchange repulsion, i.e., the interaction caused by exchange of electrons between A and B. More physically, this is the short-range repulsion due to overlap of electron distribution of A with that of B.

CT is the charge transfer or electron delocalization interaction, i.e., the interaction caused by charge transfer from occupied MO's of A to vacant MO's of B, and from occupied MO's of B to vacant MO's of A, and the higher order coupled interactions.

MIX is the coupling term which is the difference between the total SCF interaction energy ΔE_{SCF} and the sum of the above four components and accounts for higher order interaction between various components.

In addition to the above components calculated within the Hartree–Fock scheme, there is a contribution of the correlation

energy ΔE_{corr} which can further be divided into the intramolecular correlation term, CA, and the intermolecular term, CR.

$$\Delta E_{corr} = CA + CR \quad (2)$$

A part of the intermolecular correlation term CR is known as the dispersion energy, DISP.[16] This is the interaction resulting from instantaneous polarization of A and B. Approximate calculations for atomic and molecular interactions and apparent successes of Hartree–Fock calculations indicate that the effect of ΔE_{corr} is relatively unimportant for interactions of polar molecules.

In the previous papers of this series, we have used the ECDD analysis to elucidate the origin of interaction in the ground and some lower excited states of several EDA complexes. Around the equilibrium geometry of the ground state of weak n–π^* complexes such as ether ROR (a so-called n-electron donor)–carbonyl cyanide $OC(CN)_2$ (a so-called π-electron acceptor), and ether–tetracyanoethylene $(NC)_2C{=}C(CN)_2$ (a π acceptor), we found that the electrostatic interaction ES was the dominant contributor (several kcal/mol) to the stabilization, while the contribution of the charge transfer energy, CT, was not essential (of the order of 1 kcal/mol).[12] One may well call these complexes "weak electrostatic complexes". In the benzene–carbonyl cyanide complex, the dispersion energy, DISP, was found to be as important as the SCF contribution ΔE_{SCF}.[13] On the other hand, around the equilibrium geometry of the strong complex $OC{-}BH_3$, the three attractive interactions, ES, CT, and PL, are found to be of comparable magnitude and are all essential for binding of the complex.[14] This complex can be called an "electrostatic-charge-transfer polarization complex". In the even stronger borazane complexes, $H_3N{-}BH_3$ and $H_3N{-}BF_3$, ES is found to be much larger than CT and PL and is the only attractive term required to keep the complex bound.[14] These complexes are therefore "strong electrostatic complexes".

In the present paper, after the Introduction (section II), we present the results of ECDD analyses for several halogen complexes: $H_3N{-}F_2$, $H_3N{-}Cl_2$, $H_3N{-}ClF$, $CH_3H_2N{-}ClF$ (these all in section III), $H_2CO{-}F_2$ (section IV), HF–ClF (section V), and $(F_2)_2$ (section VI). The first four of these have been subjected to an MO study by Lucchase and Schaefer,[18] who found that a minimal basis set gave results which were very different from two larger basis sets: a double-ζ set and a double-ζ plus polarization set. The present ECDD analysis should clarify subtle differences in relative binding capabilities of donors such as H_3N and CH_3H_2N and of acceptors such as ClF, Cl_2, and F_2. The dramatic contrast in the effect of alkyl substitution, i.e., the large effect in the proton affinity of ammonia and amines $R_1R_2R_3N$, and the almost total absence of such an effect in the binding energy of amine–BH_3 complexes has been attributed to PL and EX; the increase in the PL stabilization and the increase in the EX repulsion upon successive alkylation cancel one another in the complex with BH_3, whereas EX repulsion does not exist in the complex with H^+, thus leaving the PL effect uncancelled.[14,15] The ECDD analysis for the present complexes is also expected to shed light on the origin of alkyl substituent effects. The $H_2CO{-}F_2$ complex has been picked as a model for well-known complexes between ketones and Br_2 and I_2.[2]

The HF–ClF complex has recently been found by Janda, Klemperer, and Novick in the molecular beam microwave spectroscopy and its structure has been determined.[19] At the present time, the non-hydrogen bonded complex of the form HF–ClF is the only form which has been observed, while its hydrogen bonded counterpart FH–FCl has gone undetected. A comparison of the stable structures in both non-hydrogen bonded and hydrogen bonded complexes is a topic of the present study. The ECDD analysis also enables a direct comparison of the origin of bonding between two forms of the complex, serving as a guide for a unified theory of EDA complexes and hydrogen bonds. The fluorine dimer, $(F_2)_2$, has been chosen as a model of another halogen dimer, $(Cl_2)_2$, which has recently been found to be a polar molecule with a dipole moment about 0.2 D or greater.[20] $(F_2)_2$ itself appears to be a polar molecule with a dipole moment on the order of 0.1 D.[21] A model of an "L" shaped or a "T" shaped dimer has been proposed for the geometry of $(Cl_2)_2$, based on the structure of the Cl_2 crystal and on the quadrupole–quadrupole interaction scheme.[20] We examine the geometry of the $(F_2)_2$ complex, employing an estimate of the dispersion energy as well as ΔE_{SCF}. The final section of the paper is a summarizing discussion (section VII) on the overall picture of the EDA interaction obtained in this series of papers.

II. Methods and Geometries

All the calculations of ΔE_{SCF} have been carried out within the closed shell LCAO-SCF approximation with the 4-31G split valence-shell basis set with recommended exponents, contraction coefficients, and scale factors.[22a] The GAUSSIAN 70 program with our own ECDD analysis routines has been used.[22b] The 4-31G basis set is flexible enough to give a reasonable estimate of the interaction energy and its components. However, it does have a tendency to exaggerate the polarity of molecules, resulting in an overestimate of the interaction energy, particularly ES.[9,11,23] When a delicate comparison of different stable geometries of a complex was required, as in the HF–ClF complex, the 4-31G** basis set which includes one set of polarization functions on each atom (a p function with the exponent $\alpha = 1.1$ for a hydrogen atom and a d function with $\alpha = 0.8$ for other atoms)[24] was adopted, in addition to 4-31G. The IBMOLH program has been used for the evaluation of integrals involving d functions.[25] This basis set, to a great extent, alleviates the problem of exaggerated polarities experienced with the less flexible 4-31G set. The calculated and experimental dipole moments of the acceptors and donors are shown in Table I.

The geometries of the monomers were taken from experimental results, unless otherwise noted. F_2, r(F–F) = 1.417 Å; ClF, r(Cl–F) = 1.628 Å; Cl_2, r(Cl–Cl) = 1.988 Å;[26] H_3N, r(N–H) = 1.0124 Å and ∠HNH = 106.67°;[27] CH_3H_2N, C_s, staggered, r(C–N) = 1.451 Å, $r(CH_s)$ = 1.109 Å, $r(CH_a)$ = 1.088 Å, ∠CNH = 110.9°, $\angle NCH_s$ = 111.7°, $\angle NCH_a$ = 110.1°, $\angle H_aCH_s$ = 108.1°, $\angle H_aCH_a$ = 108.6° (above from Me_3N),[28] and r(N–H) = 1.0124 Å (from NH_3) where H_s is on a symmetry plane and two H_a's are not; H_2CO, C_{2v}, r(C–H) = 1.102 Å, r(C=O) = 1.210 Å, ∠HCH = 121.1°;[27] HF, r(H–F) = 0.9171 Å.[29] They were assumed to be unchanged upon complex formation. Only a limited optimization of the geometry of complexes was carried out with respect to intermolecular distances and angles.

For $(F_2)_2$ the dispersion energy DISP has been estimated by the second-order perturbation scheme, as was described previously.[13]

$$\mathrm{DISP} = -4 \sum_{i}^{occ} \sum_{k}^{vac} \sum_{\mu}^{occ} \sum_{\nu}^{vac} \frac{|\langle i_A k_A | \mu_B \nu_B \rangle|^2}{E_{i\to k}{}^A + E_{\mu\to\nu}{}^B - E_0{}^A - E_0{}^B} \quad (3)$$

where $\langle i_A k_A | \mu_B \nu_B \rangle$ is a two-electron integral over the SCF-MO's of isolated molecules. Terms in the denominators such as $E_0{}^A$ and $E_{\mu\to\nu}{}^B$ are the unperturbed energies of isolated molecules in the ground and singly excited states.

The ECDD analysis has been performed with the method of Kitaura and Morokuma.[8] The definitions of energy and charge distribution components and mechanics of calculation have been summarized in one of our recent papers[14] and will not be repeated here. When an analytic potential as a function

Table I. Experimental and Calculated Dipole Moment of Monomers (in D)

	Exptl	Calcd 4-31G
NH_3	1.468[a]	2.30
ClF	2.1 ± 1.4 (Cl^-F^+)[b]	1.58 (Cl^+F^-)
	0.88[c]	
	0.81 (Cl^+F^-)[d]	
H_2O	1.85[e]	2.60
HF	1.83[f]	2.28
H_2CO	2.33[g]	3.00

[a] C. H. Townes and A. L. Schawlow, "Microwave Spectroscopy", McGraw-Hill, New York, N.Y., 1955. [b] J. J. Ewing, H. L. Tigelaar, and W. H. Flygare, *J. Chem. Phys.*, **56**, 1957 (1972). [c] R. E. Davis and J. S. Muenter, *ibid.*, **57**, 2836 (1972). [d] Reference 19. [e] T. R. Dyke and J. S. Muenter, *J. Chem. Phys.*, **59**, 3125 (1973). [f] J. S. Muenter and W. Klemperer, *J. Chem. Phys.*, **52**, 6033 (1970). [g] K. Kondo and T. Oka, *J. Phys. Soc. Jpn.*, **15**, 307 (1960).

of a geometric variable was necessary, a rational fraction was fit to the calculated data points.[14] In sections III–V, ΔE is used to mean ΔE_{SCF}.

III. Ammonia and Amine–Halogen Complexes

(A) H_3N–F_2. First we examined the interaction energy components of the H_3N–F_2 complex as a function of the intermolecular separation $R = r(N\text{–}F_a)$ as one end F_a of the fluorine molecule approaches N of NH_3 maintaining the overall C_{3v} symmetry. The results are shown in Table II.

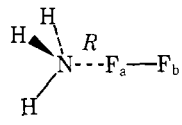

1

At the calculated equilibrium separation R_e = 3.00 Å, the electrostatic energy, ES, and the charge transfer energy, CT, are the largest contributors to the stabilization, while the polarization energy, PL, makes a minor contribution. A large ES contribution is somewhat of a surprise for a complex of a nonpolar monomer molecule. It is recognized, however, that F_2 has a permanent quadrupole (and higher multipoles) and that its interaction with a large dipole moment (and higher multipoles) of H_3N can result in a substantial ES. Our ES, which is derived from the full electron distribution rather than multipole expansion, of course includes all the multipole interactions. CT consists of the $H_3N \rightarrow F_2$ charge transfer, the $H_3N \leftarrow F_2$ back donation, and their coupling.[8] Though we have not separated these terms, presumably the charge transfer from the highest occupied N lone pair (n) orbital of NH_3 to the lowest vacant σ^* orbital of F_2 is the principal contribution to CT stabilization. This conjecture is supported by the components of the changes in the gross atomic population shown in Table III and by the plots of electron density changes in Figure 1. A charge transfer takes place from NH_3 to F_2 along the C_{3v} axis via σ orbitals. The PL effect causes a large (compared to other effects) shift of electron distribution in F_2, inducing a dipole $F_a^{+\delta}$–$F_b^{-\delta}$. The principal contribution to the PL energy, therefore, should come from the interaction of the permanent polarity of NH_3 with an induced polarity of F_2. As is seen in Figure 1, a small additional polarity is $^{-\delta'+\delta'}N\text{–}^{-\delta'+\delta'}H_3$ is induced on H_3N by a large induced polarity in F_2. EX causes a small depletion of electron density from the interaction region as is seen in Figure 1.

In order to find out which components are necessary to keep a bound complex, we have plotted, as a function of R, the truncated interaction ΔE^{tr} in which one attractive component (ES, PL, or CT) is removed. The equilibrium intermolecular separations R_e^{tr} and the energies ΔE_e^{tr} at R_e^{tr} for various truncated interaction curves are shown in Table IV. It is clear from Table IV that both ES and CT are necessary for a bound complex. This is a weak "ES–CT complex".

Table II. Energy Decomposition Analysis for the Complex H_3N–F_2 at Various Separations in kcal/mol (C_{3v} and Perpendicular Approaches)

	C_{3v} (1)				Perpendicular (2)
R, Å	2.68	3.00[a]	3.08	3.48	3.00
ΔE	−0.82	−1.05	−1.00	−0.59	0.53
ES	−1.67	−0.76	−0.65	−0.35	−0.07
EX	2.57	0.61	0.42	0.06	0.98
PL	−0.52	−0.28	−0.24	−0.12	−0.09
CT	−1.30	−0.64	−0.54	−0.18	−0.30
MIX	0.11	0.03	0.02	0.00	0.01

[a] The equilibrium R determined from a parabolic fit. The energy and its components are actual calculated values.

A deviation of the F_2 approach from the NH_3 C_{3v} axis decreases the stabilization of the complex.[18] In order to investigate the origin of this change, we examined an approach in which the F_2 molecular axis is perpendicular to the C_{3v} axes with one of the fluorine atoms, F_a, on the C_{3v} axes. The results

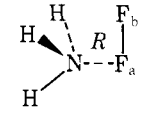

2

at R = 3.00 Å are shown in the last column of Table II. A comparison with the C_{3v} approach at the same R indicates that all the components destabilize the complex upon deviation from C_{3v}, the most notable contribution being ES, followed by EX and CT. The ES destabilization can be understood as follows. If the electron distribution is spherical around the atom F_a, the deviation should not change ES between NH_3 and F_a. Actually an F atom has two pπ electrons in each direction but only one pσ electron. Therefore the F_2 electron distribution is more dense (negative) to the direction perpendicular to the bond axis than along the axis. Therefore the electron rich N atom should prefer the axial approach. This contention is supported by calculating for F_2 the electrostatic potential $\phi(r)$, i.e., the electrostatic interaction energy when a unit positive charge (e.g., proton) is at r. The 4-31G wave function gives $\phi(r)$ = −428.6 kcal/mol at 3 Å from the closer F atom along the F_2 bond axis, and $\phi(r)$ = −443.7 kcal/mol at 3 Å from an F atom in the direction perpendicular to the bond axis. A unit positive charge is stabilized more in the perpendicular approach, and this approach is less favored for the electron rich N atom of NH_3.

NH_3 and F_2 can interact through hydrogen bonding to form a complex $H_2NH\text{–}F_2$. We have not examined such an approach for any H_3N–halogen complexes. A comparison of hydrogen bonded and non-hydrogen bonded complexes will be made for FCl–FH in section V.

(B) H_3N–ClF. This system has been chosen for comparison with H_3N–F_2 and H_3N–Cl_2; ClF has a permanent dipole whereas F_2 and Cl_2 are, of course, nonpolar. We first examined the C_{3v} complex, in which the Cl end of ClF approaches the N of the NH_3. This orientation was found to be the most favored approach.[18]

Table III. Gross Atomic Electron Population of Isolated Molecules and Its Component Changes for the Complex H_3N-F_2 (C_{3v} Approach, R = 3.00 Å)

	NH_3		F_2		
	H	N	F_a	F_b	$[H_3N \overset{(+)}{\underset{(-)}{\rightleftarrows}} F_aF_b{}^a]$
Isolated molecule	0.7078	7.8945	9.0000	9.0000	
Total change[b]	−0.0027	0.0045	−0.0337	0.0373	0.0035
EX[b]	0.0	0.0	−0.0003	0.0003	
PL[b]	−0.0021	0.0062	−0.0342	0.0342	
CT[b]	0.0	−0.0037	0.0030	0.0007	0.0036
MIX[b]	−0.0007	0.0021	−0.0023	0.0022	−0.0001

[a] A positive value indicates a net charge transfer from NH_3 to F_2 and negative from F_2 to NH_3. [b] Positive and negative values indicate an increase and a decrease, respectively, of electron population upon complex formation.

Table IV. Truncated Interaction Energy ΔE^{tr} and Equilibrium Separation $R_e{}^{tr}$ for H_3N-F_2 (C_{3v} Approach)

ΔE^{tr}	$R_e{}^{tr}$, Å	$\Delta E_e{}^{tr}$, kcal/mol
ΔE	3.00	−1.05
ΔE-ES	3.22	−0.39
ΔE-PL	3.02	−0.77
ΔE-CT	3.24	−0.50

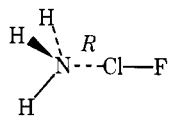

3

Table V shows the results as functions of $R = r$(N-Cl). At the calculated equilibrium R_e, the complex is highly electrostatic in nature, with a substantial additional contribution from CT. The equilibrium separation $R_e{}^{tr}$ from truncated potential energy curves, shown in Table VI, suggests that the removal of ES would make the complex only weakly bound and that the lack of CT would also have a substantial influence on the binding. Though the sign of the experimental dipole moment of Cl appears to be a subject of controversy (Table I), a comparison of these with accurate ab initio calculations by Green (1.099 D Cl^+F^- for the Hartree-Fock and 0.839 D Cl^+F^- for the CI calculation)[30] suggests that the present 4-31G dipole is of the correct sign but the magnitude is overestimated. Even if such an overestimation is taken into account, the complex can still be characterized as a "ES-CT or ES complex" of intermediate strength.

A comparison of this complex with another "ES-CT complex", H_3N-F_2, which is very weak, is interesting. The chlorine atom has a bulkier electron distribution, i.e., a larger van der Waals radius, than the fluorine atom. This is reflected in different energy components in the two complexes at about the same separation R, e.g., 3.00 and 3.08 Å for H_3N-F_2 in Table II and 3.05 Å for H_3N-ClF in Table V. Because of a bulkier electron cloud, the ClF complex has a larger EX repulsion and also larger CT and PL attractions than the F_2 complex. At such a large distance, however, ES is the predominant term; the H_3N-ClF complex is an ES complex. The strong ES attraction pulls the molecules closer together, resulting in a much smaller R_e. At a smaller R, the relative importance of CT increases rather drastically, making this complex an "ES-CT complex" of intermediate strength.

The results of electron population decomposition and the plots of electron density components near the calculated R_e are shown in Table VII and Figure 2, respectively. Since R_e is smaller, an order of magnitude larger charge transfer takes place in H_3N-ClF than in H_3N-F_2 (Table III and Figure 1). CT is from NH_3 to ClF along the C_{3v} axis through the σ orbitals. This can be seen clearly in ρ_{CT} of Figure 2 with the transferred charge accumulating in the intermolecular region. However, EX and PL of ClF both shift the electron cloud away from the interaction region; the overall $\Delta\rho$ shows a depletion of electron distribution between N and Cl. A large polarization of NH_3 as well as ClF is observed in ρ_{PL}.

Table V. Energy Decomposition Analysis for the Complex H_3N-ClF at Various Separations in kcal/mol (C_{3v} and Perpendicular Approaches)

	C_{3v} (3)			Perpendicular (4)	
R, Å	2.25	2.65	2.717[a]	3.05	2.717
ΔE	−4.68	−8.16	−8.23	−6.43	8.50
ES	−36.86	−12.96	−11.18	−6.23	−5.32
EX	47.53	10.02	7.41	2.02	15.32
PL	−3.71	−1.23	−1.05	−0.55	−0.38
CT	−12.62	−4.22	−3.59	−1.77	−1.26
MIX	0.98	0.24	0.19	0.10	0.13

[a] The equilibrium R and energy components determined for a parabolic fit.

Table VI. Truncated Interaction Energy ΔE^{tr} and Equilibrium Separation R^{tr} for H_3N-ClF (C_{3v} Approach)

ΔE^{tr}	$R_e{}^{tr}$, Å	$\Delta E_e{}^{tr}$, kcal/mol
ΔE	2.72	−8.23
ΔE-ES	2.94	−1.06
ΔE-PL	2.79	−7.36
ΔE-CT	2.88	−5.72

We also examined the approach in which the ClF axis staggered with respect to the NH_3 is perpendicular to the C_{3v} axis, with the Cl atom on the C_{3v} axis (Table V). This approach

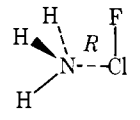

4

is strongly repulsive at $R = r$(N-Cl) = 2.717 Å. When compared with the C_{3v} approach, this unstability is mainly due to an increase in the EX repulsion and a decrease in the ES stabilization. The misalignment of permanent dipoles qualitatively explains the decrease in ES. Despite a polarity Cl^+F^-, the electron density on the chlorine atom is more dense along the π axis (because π orbitals are saturated) than the σ axis, as was discussed for the F_2 complex. As a result, the EX repulsion is probably larger in the perpendicular approach than the C_{3v} approach.

Table VII. Gross Atomic Electron Population of Isolated Molecules and Its Component Changes for the Complex H_3N-ClF (C_{3v} Approach, R = 2.65 Å)

	NH_3		ClF		$H_3N \underset{(-)}{\overset{(+)}{\rightleftarrows}} ClF^a$
	H	N	Cl	F	
Isolated molecule	0.7078	7.8945	16.6050	9.3950	
Total change[b]	−0.0234	0.0316	−0.0328	0.0713	0.0385
EX[b]	0.0003	−0.0010	−0.0055	0.0055	
PL[b]	−0.0201	0.0604	−0.0470	0.0470	
CT[b]	0.0	−0.0350	0.0303	0.0047	0.0349
MIX[b]	−0.0036	0.0072	−0.0106	0.0141	0.0036

[a] A positive value indicates a net charge transfer from NH_3 to ClF and negative from ClF to NH_3 [b] Positive and negative values indicate an increase and a decrease, respectively, of electron population upon complex formation.

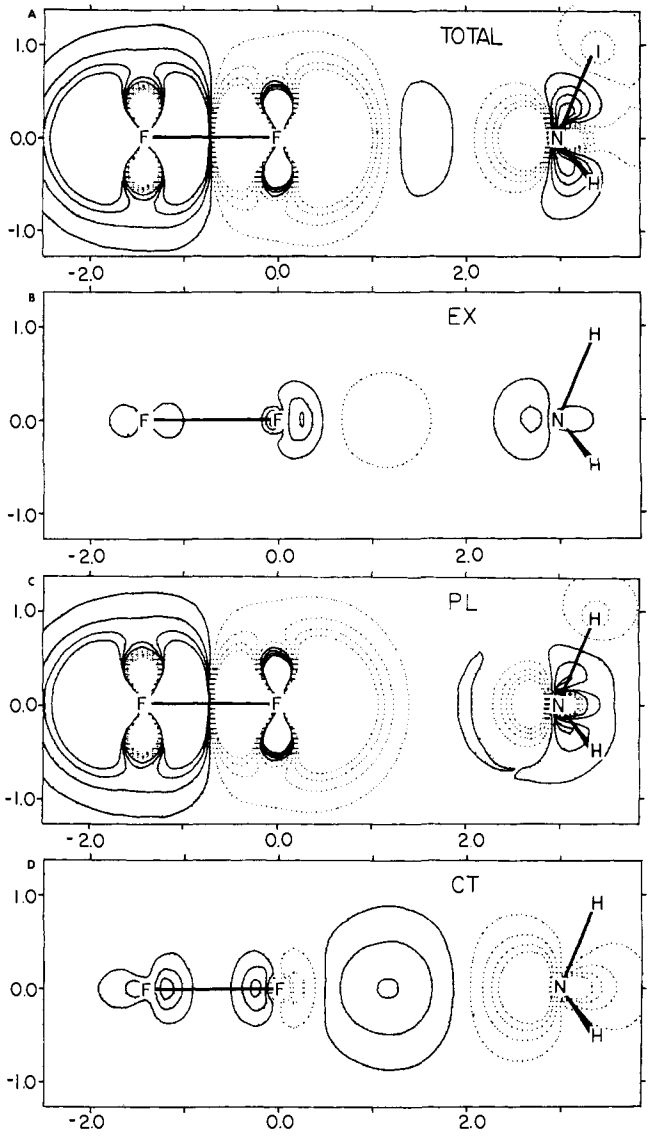

Figure 1. Component electron density maps for the complex H_3N-F_2 at r(N-F) = 3.00 Å in the C_{3v} approach. Full lines indicate density increases and dotted lines indicate decreases. Contours are successively ±1, ±3, ±5, ±7 × 10^{-4} (Bohr^{-3}). The coordinates are in Å, relative to the inner F atom, and plotting is made for the FFNH plane.

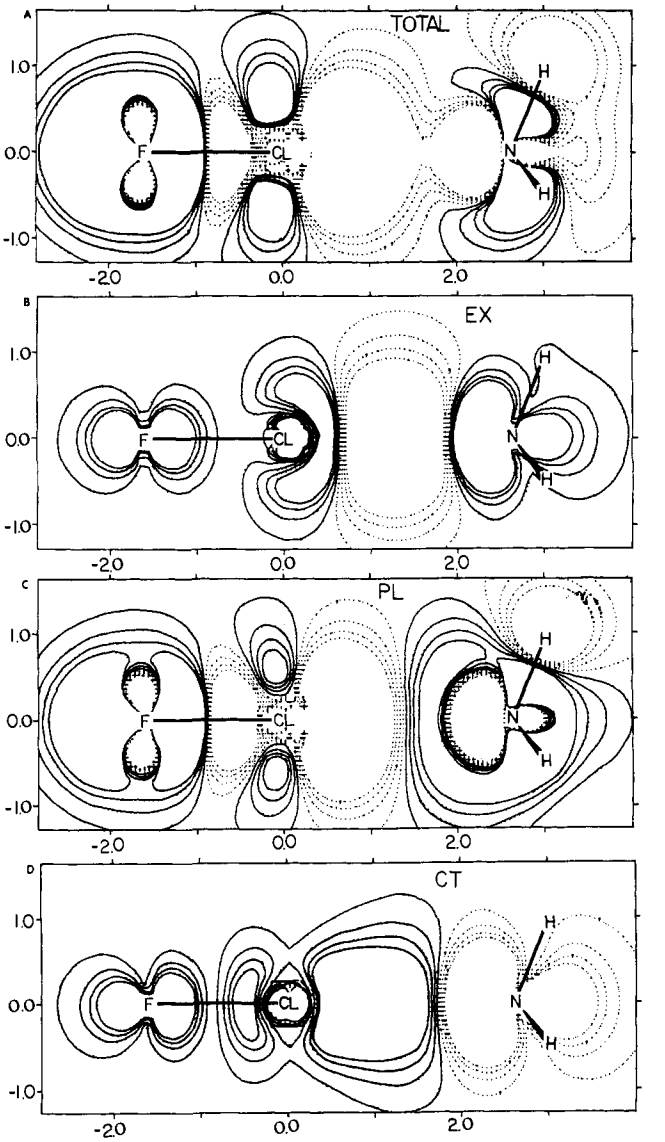

Figure 2. Component electron density map for the complex H_3N-ClF at r(N-F) = 2.65 Å in the C_{3v} approach. The coordinates are relative to Cl and plotting is made for the FClNH plane. See Figure 1 for other details.

Table VIII shows the results of energy decomposition as functions of $R = r$(N-F) for a C_{3v} complex in which the F end of ClF approaches N of NH_3. The complex was found to be unbound. This is, in principle, due to the repulsive ES interaction, whereas PL, EX, and CT components are of compa-

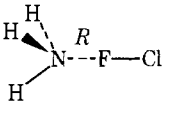

5

Table VIII. Energy Decomposition Analysis for the Complex H_3N-FCl (**4**) at Various Separations in kcal/mol (C_{3v} Approach)

	R, Å		
	2.65	3.05	3.45
ΔE	4.55	2.31	1.59
ES	2.84	2.46	1.82
EX	3.30	0.58	0.08
PL	−0.58	−0.28	−0.14
CT	−1.11	−0.47	−0.17
MIX	0.11	0.02	0.00

rable magnitude with those in the H_3N-F_2 complex (Table II).

(C) CH_3H_2N-ClF and *N*-Methyl Substituent Effect. As was discussed in section I, the *N*-methyl substituent effect on the energy of the H_3N-BH_3 complex formation is in marked contrast with the analogous effect on the proton affinity of NH_3. Lucchese and Schaefer compared the difference in the complexing ability of NH_3 and $N(CH_3)_3$ with F_2, ClF, or Cl_2 employing the minimal STO-3G basis set.[18] Since this set predicts the polarity Cl^-F^+ which is opposite to that attained from both better theoretical calculations and the recent experiment results discussed in section IIB, and since this set also has a tendency to overestimate the CT contribution, the interpretations obtained from their calculation are questionable.

The second column of Table IX shows the energy components for the H_3N-ClF complex at the calculated equilibrium (C_{3v}) geometry and their differences in parentheses between CH_3H_2N-ClF, **6**, and H_3N-ClF at the same geometry. The

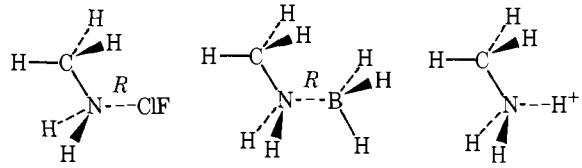

6 **7** **8**

N-methyl substitution lowers the stabilization energy of the complex by a small amount. This is consistent with previous STO-3G calculations but is in the opposite direction and of much smaller magnitude than the change in ΔH observed in solution for amine-iodine complexes.[31] The disagreement could be either due to the deficiency of the present theory or due to the solvent effect. One may note that molecular orbital calculations for the methyl substituent effect[15] on the proton affinity of amines agree well with the gas phase experiment which is substantially different from the experiment in solution.[32] The proton affinity of amines in solution is known to change in the order:

$$NH_3 < RNH_2 \cong R_2NH > R_3N$$

whereas in the gas phase the proton affinity monotonically increases in the order:[32]

$$NH_3 < RNH_2 < R_2NH < R_3N$$

The energy decomposition indicates that the decrease in the stabilization of the H_3N-ClF complex upon methylation is principally due to an increase in the EX repulsion, supplemented by a decrease in the ES stabilization. These effects are partially negated by an increase in the CT stabilization. Table IX also summarizes the calculated *N*-methyl substituent effects for the H_3N-BH_3, **7**, and the H_3N-H^+, **8**, complex. These two complexes show an additional stabilization upon methylation, in contrast to the H_3N-ClF case. The ratio of the

Table IX. A Comparison of Interaction Energy Components and *N*-Methyl Substituent Effects between Various Complexes at Equilibrium Geometry in kcal/mol

	H_3N-ClF (**6**)	H_3N-BH_3 (**7**)[a]	H_3N-H^+ (**8**)[b]
R, Å	2.717	1.705	1.02
ΔE	−8.23	−44.7	−221.9
	(0.29)[c]	(−0.8)	(−8.5)
ES	−11.18	−92.9	−99.8
	(0.32)	(−1.2)	(3.3)
EX	7.41	86.9	0.0
	(0.53)	(4.4)	(0.0)
PL	−1.05	−17.2	−27.4
	(0.02)	(−5.0)	(−12.8)
CT	−3.59	−27.1	−88.3
	(−0.57)	(−1.4)	(−3.4)
MIX	0.19	5.6	−6.5
	(−0.01)	(2.4)	(4.4)

[a] Reference 14. [b] Reference 15. [c] The numbers in parentheses are the difference between the CH_3H_2N complex and the H_3N complex. A negative number indicates that the CH_3H_2N complex is more stable, and vice versa.

difference in the stabilization energy between the CH_3H_2N and the H_3N complex versus the stabilization energy of the H_3N complex should provide a relative guide for the magnitude of the methyl substituent effect. The ratio is 4, 2, and 4% for the complex with ClF, BH_3, and H^+, respectively. The substituent effect for H_3N-BH_3 is indeed found experimentally to be very small in the gas phase.[33] An increase in the CT stabilization is common to all three complexes and can probably be attributed to the lowering of the donor's experimental ionization potential (234.1 kcal/mol for NH_3 to 206.8 kcal/mol for H_3CNH_2)[34] or, correspondingly, the increase in the donor's calculated highest occupied MO energy (−252.5 for NH_3 to −233.0 kcal/mol for H_3CNH_2 in the present calculation). The decrease in the ES stabilization is probably due to a small increase in the electron population on the N atom (7.89 for NH_3 to 7.81 for H_3CNH_2 in the present calculation). The H_3NH^+ case is in accord with the present result, but the H_3N-BH_3 complex shows an opposite trend. This anomaly is due to the fact, presumably, that the H_3 group of BH_3 can also influence the change in ES. The increase in EX is noted both for this complex and H_3N-BH_3 while it does not exist in the H_3N-H^+ complex because the proton does not have an electron. The increase in EX is presumably due to the interaction of the CH_3 group with the acceptor electrons. It is extremely interesting to note among these three complexes differences in which term is the primary contribution to the total stabilization, as well as differences in dominant terms for the methyl substituent effect. The results are summarized as follows:

(a) H_3N-ClF: stabilization, ES supplemented by CT; Me substitution, destabilization (EX, cancelled almost evenly by CT, supplemented by ES; components of order of 0.5 kcal/mol).

(b) H_3N-BH_3: stabilization, ES; Me substitution, small stabilization (PL, cancelled mostly by EX; components of order of 5 kcal/mol).

(c) H_3N-H^+: stabilization, ES and CT; Me substitution, stabilization (PL; components of order of 10 kcal/mol).

(D) H_3N-Cl_2. The H_3N-Cl_2 complex will provide a reasonable form of comparison with H_3N-F_2 in regard to the size of electron clouds of the acceptor molecule as well as with H_3N-ClF in regard to the polarity of the acceptor. A calculation was carried out for H_3N-Cl_2 in a C_{3v} (collinear NCl_aCl_b) geometry at $R = r(N\text{-}Cl_a) = 2.93$ Å, the optimal geometry by Lucchese and Schaefer in a double-ζ basis set.[18] The results are $\Delta E = -2.89$, ES = −3.98, EX = 3.94, PL =

Table X. Energy Decomposition Analysis for the Complex H_2CO-F_2 (**9**) at the Various Separations in kcal/mol[a]

	R, Å		
	2.60	2.90	3.20
ΔE	−0.44	−0.68	−0.46
ES	−0.86	−0.42	−0.26
EX	1.43	0.32	0.06
PL	−0.17	−0.10	−0.06
CT	−0.92	−0.50	−0.22
MIX	0.08	0.02	0.00

[a] A parabolic fit of these three points gives R_e = 2.907 Å.

−0.81, CT = −2.30, and MIX = 0.26 kcal/mol. In comparison with the results in Table II for H_3N-F_2, one finds that, though R_e is similar, the complex Cl_2 is stronger with all the components several times larger than their counterparts in the F_2 complex. The most notable increases are observed for EX (seven times with respect to the F_2 complex at 3.00 Å) and ES (five times). Since the Cl_2 valence electron cloud is more widely spread out, the electron donor molecule can penetrate deeper in the cloud resulting in a larger ES, CT, as well as PL before it feels the very steep wall of EX repulsion. A comparison with Table V shows that the increase in the stabilization in the H_3N-ClF complex relative to the H_3N-Cl_2 complex at the same distance (2.93 Å) is principally due to a twofold increase in ES, partially negated by a small increase in the EX repulsion. Both changes may be attributed to an increase in the electron density on the chlorine atom.

Summarizing H_3N-halogen compiexes, one may call H_3N-ClF "an ES complex" of an intermediate strength since the contribution of the next largest term CT is only 30% of ES. H_3N-Cl_2 and H_3N-F_2 are both "weak ES-CT complexes" with the CT contribution more than a half of ES.

IV. The H_2CO-F_2 Complex

As a model for another series of weak halogen complexes we studied the complex between H_2CO and F_2. Concordant with the geometry of the acetone-Br_2 complex in the crystal,[35] F_2 was assumed to approach the O atom of H_2CO collinearly within the H_2CO molecular plane with a COF angle of 120° (**9**). Table X summarizes the results of an energy decomposi-

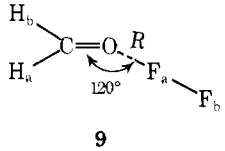

9

tion as a function of $R = r(O\text{-}F_a)$. The complex is one of the most weakly bound systems which we studied in the present paper. A comparison with the H_3N-F_2 complex (Table II) is of particular interest, since both are weak complexes. The equilibrium intermolecular separation $R = r(O\text{-}F) = 2.91$ Å for H_2CO-F_2 is smaller than $R = r(N\text{-}F) = 3.00$ Å for H_3N-F_2, even though the former is a weaker complex. This is due to the smaller size of electron cloud on O than on N and consequently a smaller EX repulsion for the former complex at the same R. This same factor is also responsible for a smaller CT attraction for H_2CO-F_2. The net charge on N of NH_3 is −0.89 (Table III) and is larger than that on O of H_2CO (−0.48 in Table XI). Though the dipole moment of NH_3 is smaller than that of H_2CO (Table I), one expects that NH_3 will give rise to a larger ES interaction than H_2CO, because the nearest charge-charge interaction is more important than the dipole-dipole interaction in determining the global ES. This is indeed what is found as is evident from a comparison of Tables II and X at the same distance. Overall, each component of the H_2CO complex is about a half or two-thirds as large as that of the NH_3 complex. Truncated potential energy ΔE^{tr} plots indicate that both ES and CT make significant contributions to the binding. Therefore, this complex as well as H_3N-F_2 may be called a weak "ES-CT complex". The population analysis in Table XI for H_2CO-F_2 shows a smaller charge migration for each component than for H_3N-F_2 at a somewhat larger distance (Table III). The polarization of H_2CO by F_2 causes the migration of charge from O to the CH_2 group. The separate π and σ population changes by CT indicate that the contribution of π CT is negligible. This is primarily because R_e is so large (2.91 Å) that the π-type overlap between π orbitals is not significant.

V. ClF-HF and FCl-FH. Hydrogen Bonded and Antihydrogen Bonded Complexes

As was discussed briefly in section I, a very recent study using microwave and radio frequency spectroscopy with a nozzle molecular beam electric resonance technique has determined the structure and dipole moment of a weakly bound non- or anti-hydrogen bonded complex FCl-FH.[19] The structure **10** has the following parameters: $r(F\text{-}Cl) = 2.7744$

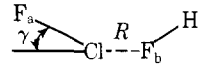

10

Å, $\angle ClF_bH = 115 \pm 5°$, $\gamma = \pi - \angle F_bClF_a = 4.94°$ (if planar), and the unknown azimuthal angle is set equal to 0. Observed dipole moments of the complex for three isotopic combinations have been used to deduce that the sign of the dipole moment of ClF is Cl^+F^-. So far the hydrogen bonded counterpart FCl-HF has gone undetected. This system provides a unique opportunity to compare ECDD analyses of hydrogen bonded and non-hydrogen bonded structures within a single complex.

(A) Geometry Optimization. It is of interest to determine whether calculations of the present level will yield geometrical results concordant with the experiment. A geometry optimization is carried out with the restriction that the ClF molecule and the F_b atom of HF are collinear, a restriction rationalized by the fact that the experimental value of γ is small. A series of calculations as functions of $R = r(F_b\text{-}Cl)$ and $\angle ClF_bH$ in Table XII give the optimized geometry as $R = 2.73_7$ Å (±0.027 Å, ±0.08 Å) and $\angle ClFH = 141°$ (±6°, ±15°). The error bounds are given arbitrarily for the energy difference of 0.006 and 0.06 kcal/mol, respectively, to illustrate roughly the flatness of the curve. In order to examine the effect of the non-linearity of F_b, Cl, and F_a, three additional calculations with $\gamma = \pi - \angle F_bClF_a = 10°$ are carried out, as are shown in the last three rows of Table XII. The collinear interaction is favored, but for the same error bounds as above, $\gamma = 0$ (±2°, ±7°) for the eclipsed conformation, implying a small deviation is indeed possible if a more extensive search is made. The calculated geometry is in reasonable agreement with the experiment. Past experiences for $(H_2O)_2$ and $(HF)_2$ suggest that the ClF_bH angle is a quantity rather sensitive to the basis set and hard to predict accurately.[1b,6b] The inversion barrier for the FH proton is calculated to be only about 0.14 kcal/mol. The absolute value of this number is not reliable, since it depends strongly on the optimized $\angle ClFH$ angle 141° which is in poor agreement with experiment 115 ± 5°. However, one may say qualitatively that it is smaller than the corresponding barrier in $(HF)_2$, where the 4-31G value is 0.35 kcal/mol with $\angle HFH$ = 135° vs. experimental 119 ± 5°.

After a reasonable geometry of the anti-hydrogen bonded complex has been obtained, we turned our attention to the hydrogen bonded complex, **11**. A limited geometry optimiza-

Table XI. Gross Atomic Electron Population of Isolated Molecules and Its Component Charges for the Complex H_2CO-F_2 (R = 2.90 Å[a])

	H_2CO				F_2		$H_2CO \overset{(+)}{\underset{(-)}{\rightleftarrows}} F_aF_b$
	H_a	H_b	C	O	F_a	F_b	
Isolated molecules	0.8447	0.8447	3.8267	8.4839	0.0	0.0	
Total change	−0.0017	−0.0017	−0.0015	0.0035	−0.0200	0.0214	0.0014
EX	0.0	0.0	0.0	0.0	−0.0001	0.0001	
PL	−0.0013	−0.0014	−0.0013	0.0038	−0.0200	0.0199	
CT	0.0001	−0.0001	0.0001	0.0015	0.0014	0.0	0.0015
MIX	0.0005	−0.0002	−0.0003	0.0012	−0.0013	0.0013	−0.0001

[a] For sign conventions, see Table III.

Table XII. Geometry Optimization for the FCl-FH Complex **10**

r(Cl-F_b), Å	∠ClF_bH, deg	Total energy[a]
2.708	115	−0.101 667
2.758	115	−0.101 672
2.808	115	−0.101 615
2.858	115	−0.101 512
2.7369	115	−0.101 678
2.7369	135	−0.102 050
2.7369	155	−0.101 965
2.7369	180	−0.101 833
2.7369	141.27	−0.102 050
2.7369	141.27 (up 10)[b]	−0.101 841
2.7369	141.27 (down 10)[b]	−0.101 571
2.7369	141.27 (back 10)[b]	−0.101 714

[a] The entry −0.101 667, for instance, means the total energy −658.101 667 hartrees. [b] Structures with nonlinear F_aClF_b. In all cases $\gamma = \pi - \angle F_bClF_a = 10°$. Azimuthal angles are 0° (eclipsed F_aClF_bH) for "up", 180° (staggered) for "down", and 90° (the F_aClF_b plane perpendicular to the ClF_bH plane) for "back", respectively.

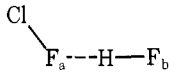

11

tion was carried out. Since the linear hydrogen bond is usually preferred, F_a, H, and F_b were assumed to be collinear. A series of calculations as functions of $R = r(F_a\text{-}H)$ and ∠HF_aCl, as shown in Table XIII, yields the following prediction for the equilibrium hydrogen bonded geometry with the 4-31G set. $r(F_a\text{-}H) = 1.86_4$ Å, ∠ClF_aH = 143°, ΔE = −4.7 kcal/mol. Since $r(F_b\text{-}H)$ = 0.917 Å was assumed, this gives $r(F_a\text{-}F_b)$ = 2.78 Å. The barrier for inversion of the Cl atom is only 0.16 kcal/mol. As was mentioned above the ClF_aH angle and the inversion barrier are quantities sensitive to the basis set and full geometry optimization and hence are difficult to accurately evaluate. Nevertheless one might guess that the hydrogen bonded complex will be extremely floppy. The calculated geometry of this complex may be compared with that of $(HF)_2$. Experimentally, r(F-F) = 2.79 Å, ∠HFH = 119 ± 5°;[36] and theoretically optimized with the present basis set in the same fashion as in this section, r(F-F) = 2.71 Å, ∠HFH = 135°, ΔE = −7.6 kcal/mol, and barrier for inversion = 0.35 kcal/mol. In a qualitative comparison with $(HF)_2$, the ClF-HF complex is a weaker complex with a smaller $|\Delta E|$ and a larger r(F-F) and has a smaller barrier for inversion of the external atom, with a less acutely bent geometry. Taking into account the error of the 4-31G results, we might make the following corrected predictions of the ClF-HF geometry: $r(F_a\text{-}F_b) \sim 2.86$ Å, ∠ClF_aH = 130°.

Though a definite determination has not been made, it appears that both hydrogen bonded and anti-hydrogen bonded complexes are local minima on the potential energy surface.

Table XIII. Geometry Optimization for the ClF-HF Complex **11**

$r(F_a\text{-}H)$, Å	∠ClF_aH, deg	Total energy[a]
1.867	180	−0.103 913
1.917	180	−0.103 866
1.967	180	−0.103 757
1.8546	180	−0.103 911
1.8546	155.93	−0.104 069
1.8546	150	−0.104 124
1.8546	140	−0.104 160
1.8546	130	−0.104 034
1.8639	142.81	−0.104 165

[a] The entry is the total energy + 658 hartrees.

Table XIV. Interaction Energy and Its Components for FCl-FH and ClF-HF at the 4-31G Optimized Geometries (kcal/mol)

	4-31G		4-31G**	
	Anti-H bonding	H bonding	Anti-H bonding	H bonding
ΔE	−3.35	−4.68	−3.23	−2.54
ES	−3.62	−4.81	−2.96	−2.70
EX	1.82	2.92	1.72	3.00
PL	−0.22	−0.73	−0.24	−0.77
CT	−1.41	−2.07	−1.87	−2.26
MIX	0.08	0.02	0.12	0.19

(B) Polarized Basis Set. At the present level of calculation, the hydrogen bonded form seems to be about 1.3 kcal/mol more stable than the anti-hydrogen bonded form. However, the difference is rather small yielding this somewhat inconclusive result. Since the 4-31G set exaggerates the ES contribution, the relative energy of the two forms may be dependent on the choice of basis set. In order to examine this possibility, calculations were carried out with a 4-31G** basis set at the 4-31 optimized geometries of both forms. This set has a p function on the hydrogen atom and a d function on the other atoms to facilitate the angular polarization of atomic orbitals.[24] The results of the calculations are shown in Table XIV. The relative stability of the two forms has reversed! In the 4-31G** basis set, the anti-hydrogen bonded complex is found to be about 0.7 kcal/mol more stable than the hydrogen bonded complex. Still, the energy difference between the two forms is not large enough to be conclusive. Slight changes caused by the geometry reoptimization, a larger basis set, or the contribution of the dispersion energy and other correlation energy terms may, once again, tip the balance. If the two forms are indeed of nearly equal stability, there is a chance of finding

Table XV. Energy Components for Nonlinear FCl-FH around Calculated Equilibrium[a]

		Configuration		
	Linear	Up	Down	Back
Azimuthal angle, deg		0	180	90
ΔE	−3.35	−3.22	−3.05	−3.14
ES	−3.62	−3.65	−3.42	−3.54
EX	1.82	1.94	1.90	1.92
PL	−0.22	−0.23	−0.20	−0.21
CT	−1.41	−1.35	−1.41	−1.38
MIX	0.08	0.07	0.08	0.07

[a] $r(Cl-F_b) = 2.7369$ Å, $\angle ClF_bH = 141.27°$, $\gamma = \pi - \angle F_bClF_a = 10°$, except for linear configuration for which $\gamma = 0$. See text for description of configuration.

both or either one of them depending on the experimental condition. The present experimental situation that only the anti-hydrogen bonded species has been found[19] could mean either that this is much more stable than the other complex or that the nozzle beam condition selectively formed this complex.

Table XIV indicates that the difference between 4-31G and 4-31G** results is principally due to the difference in ES, compensated slightly by CT. The decrease in ES attraction upon going from 4-31G to 4-31G** is more pronounced for the hydrogen bonded complex (+2.1 kcal/mol) than for the anti-hydrogen bonded complex (+0.7 kcal/mol). Since the 4-31G** basis set partially corrects the 4-31G's overestimate of ES, the 4-31G** results are more likely to be correct.

(C) Energy and Charge Distribution in Decomposition Analyses. The effects of nonlinearity on the anti-hydrogen bonded complex were examined. Table XV shows energy decomposition results for the complex around $r(Cl-F_b) = 2.7369$ Å and $\angle ClF_bH = 141.27°$, the calculated equilibrium geometry. In all cases, $\gamma = \pi - \angle F_bClF_a = 10°$, and the azimuthal angle was taken to be 0° (eclipsed F_aClF_bH) for "up", 180° (staggered) for "down", and 90° (F_aClF_b plane perpendicular to the ClF_bH plane) for "back" configuration, respectively. The unstability of "down" and "back" configurations is principally due to a decrease in ES stabilization and an increase in EX repulsion. The "up" configuration is unfavored due to an increase in EX as well as a substantial loss in CT. Any deviation of F_a from the linearity will increase the overlap of electron clouds, leading to an increase in EX. The change in ES can be understood in terms of the polarity: $F^{-\delta}Cl^{+\delta}$ and $F^{-\delta'}H^{+\delta'}$. The loss of CT in the "up" configuration can be attributed to a loss of overlap between the π and σ electron cloud of the donor and the acceptor's σ^* orbital, which is concentrated along the F_aCl axis.

We have also performed energy decomposition analysis for both FCl-FH and ClF-HF complexes at the 4-31G level as a function of the intermolecular separation. For FCl-FH a geometry with a collinear F_bClF_a and $\angle ClF_bH = 115°$, which is similar to the experiment, was used. For ClF-HF a collinear ($C_{\infty v}$) geometry was assumed. Table XVI shows the results. From Tables XVI and XIV, one finds that the anti-hydrogen bonded complex near the equilibrium is principally stabilized by ES, with a substantial supplement of CT. For the hydrogen bonded complex at the equilibrium R the stabilization is almost equally shared by ES and CT in the 4-31G** basis set. Employing the 4-31G basis set the CT contribution is of the equally shared by ES and CT in the 4-31G** basis set. Employing the 4-31G basis set the CT contribution is of the same magnitude as with the 4-31G** set, while the ES contribution is still larger and appears to be overestimated. In light of this evidence one may say that the hydrogen bonded complex is a weak ES-CT complex, whereas the anti-hydrogen bonded complex is a weak ES or ES-CT complex. The component which displays the largest difference between the two forms of the complex is EX. For a comparable Cl-F and F-F distance, the HF proton in the hydrogen bonded complex is more deeply buried in the electron cloud than any atom of the anti-hydrogen bonded complex, presumably causing a large EX. PL contribution is of secondary importance in either complex but is larger in the hydrogen bonded complex, presumably again because the proton within a short distance exerts the largest influence on the electron clouds of the partner.

The electron density distribution decomposition provides an alternative and visual insight to the origin of bonding. Figures 3 and 4 are component electron density maps for FCl-FH and ClF-HF, respectively. Table XVII shows the corresponding component electron population for both complexes. The decomposition analysis reveals all the characteristics familiar with other hydrogen bonded and non-hydrogen bonded complexes studied by the authors (section III and ref 10 and 14), with some exceptions. EX removes the electron cloud from the interaction region, but its effect is rather small. ClF-HF experiences a larger EX electron shift than FCl-FH, which is reflected in EX repulsion in Table XIV. PL is the largest contributor to the electron redistribution, though its contribution to energy is small. PL gives rise to a polarity $Cl^{-\delta+\delta}F$- - -$H^{-\delta+\delta}F$ in ClF-HF and $F^{+\delta-\delta}Cl$- - -$F^{+\delta-\delta}H$ in FCl-FH. The PL charge redistribution as well as the PL energy is larger for ClF-HF than for FCl-FH. CT transfers electrons from the terminal atom of the electron donor to the terminal atom of the acceptor like Cl ← F in FCl-FH and F → H in ClF-HF, causing a charge buildup in the intermolecular region. Table XVII indicates that MIX plays a very important role in redistribution of charge although its contribution to energy is totally negligible (Table XIV). MIX, which is in principle the coupling between CT and PL, apparently collaborates with PL and shifts the electrons, which have just been transferred by CT from the electron donor to the terminal atom of the electron acceptor, toward the further end of the acceptor. So, when CT + MIX is examined as a whole, the

Table XVI. Energy Components for FCl-FH, ClF-HF, and $(HF)_2$ as Functions of Intermolecular Separation (kcal/mol)

	FCl-FH[a]				ClF-HF[b]				$(HF)_2$[c]
R, Å	2.474	2.774	2.808	3.074	1.7	1.917	2.0	2.3	1.873
ΔE	−2.2	−3.10	−3.11	−2.5	−4.1	−4.40	−4.36	−3.5	−7.4
ES	−5.8	−3.1	−2.9	−2.0	−5.9	−4.2	−3.8	−2.7	−7.3
EX	6.6	1.7	1.4	0.4	5.5	2.2	1.4	0.3	2.6
PL	−0.3	−0.1	−0.1	−0.1	−1.4	−0.8	−0.6	−0.3	−0.5
CT	−2.9	−1.7	−1.5	−0.9	−2.7	−1.8	−1.5	−0.9	−2.1
MIX	0.2	0.1	0.1	0.0	0.3	0.1	0.1	0.0	−0.0

[a] Collinear FClF and $\angle ClFH = 115°$ assumed. $R = r(Cl-F)$. [b] Collinear ClFHF assumed. $R = r(F-H)$. [c] Collinear HFHF assumed. $R = r(F-H)$.

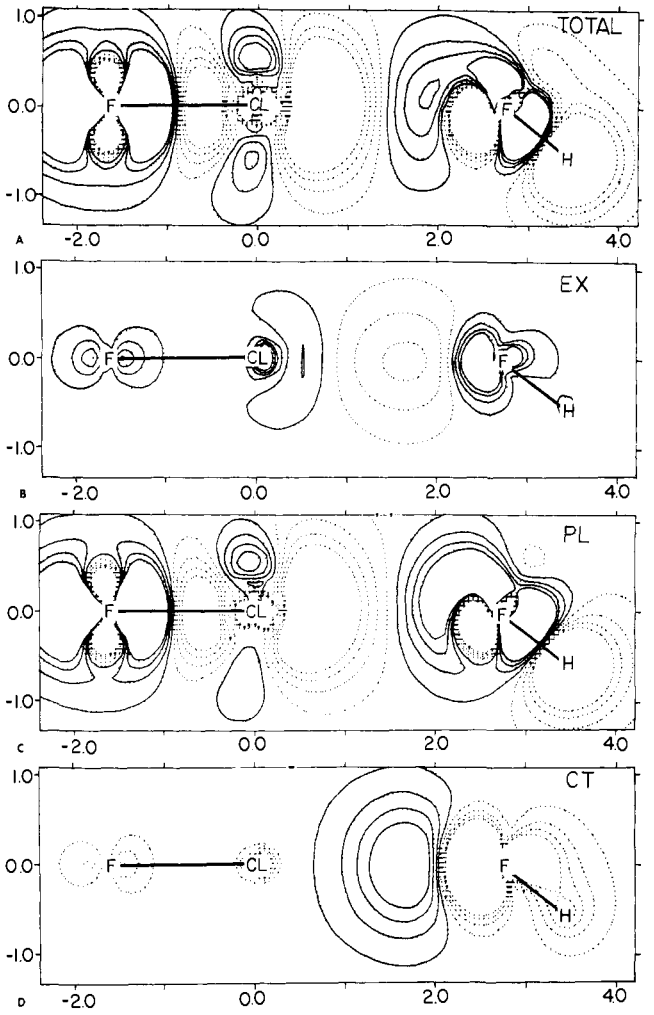

Figure 3. Component electron density map for the anti-hydrogen bonded complex FCl-FH at r(Cl-F) = 2.737 Å, ∠HFCl = 141°, and $\gamma = \pi -$ ∠FClF = 0. The coordinate origin is F of FH, and plotting is made for the molecular plane. See Figure 1 for other details.

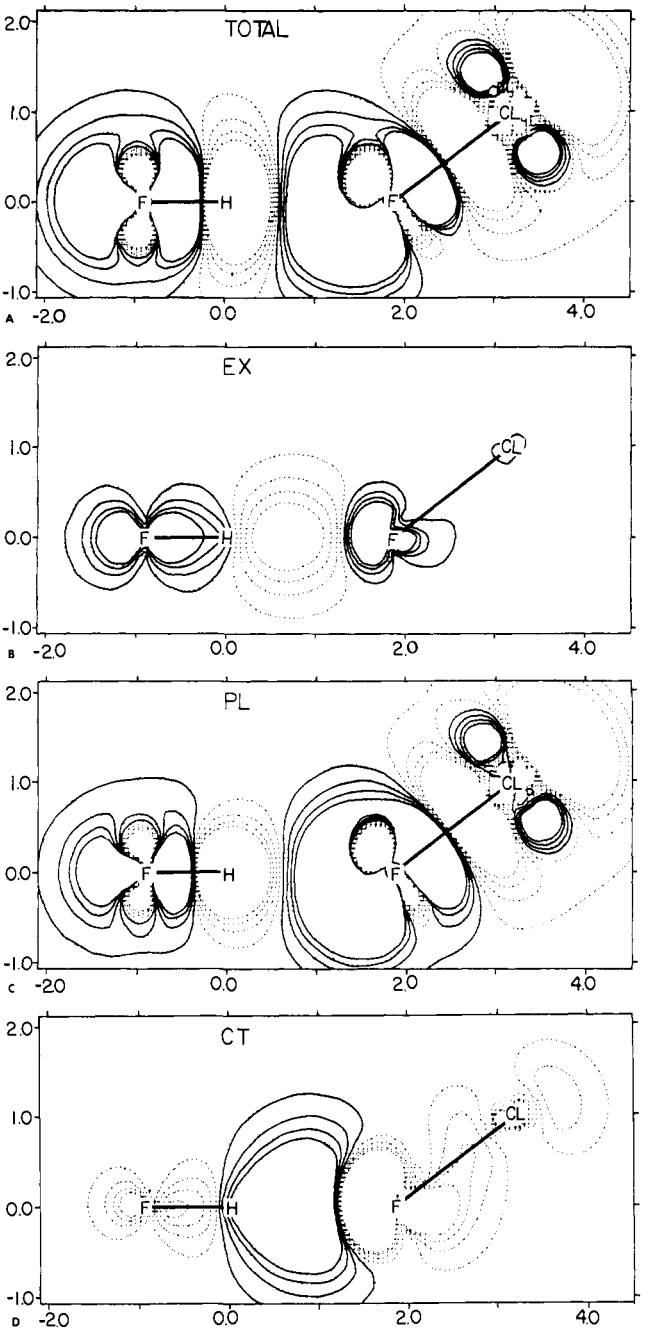

Figure 4. Component electron density map for the hydrogen bonded complex ClF-HF at r(F-H) = 1.864 Å, ∠ClFH = 143°, and ∠FHF = 180°. The coordinate origin is H of HF, and a plotting is made for the molecular plane. See Figure 1 for other details.

electron appears to migrate from the donor to the further end of the acceptor.[10] The charge decomposition as well as the energy decomposition (Table XIV) analyses confirm that the hydrogen bonded complex ClF–HF is more strongly interacting, i.e., its individual energy and charge components are larger than those of the anti-hydrogen bonded complex FCl–FH, even though the total interaction energy is comparable between the two complexes.

Table XVIII shows the change in the dipole moment and its components at the experimental geometry for FCl–FH. There is about 10% (0.3D) enhancement of the dipole moment upon complex formation. Though the absolute value of μ is an overestimate (2.3 D experimental[19] vs. 3.6 D calculated with this basis set), one can still note that the enhancement is mainly due to PL, i.e., the induced dipole moment by the permanent multipoles, supplemented by CT and MIX. This trend is consistent with the charge redistribution analysis presented above.

VI. $(F_2)_2$

As was briefly discussed in section I, the chlorine dimer $(Cl_2)_2$ is established to be a polar complex with a dipole moment ≥0.2 D. Two models have been proposed as a possible structure of the polar complex. An "L" shaped structure is derived from the structure of the Cl_2 crystal. A "T" shaped structure is favored for the long-range quadrupole–quadrupole interaction.[20] $(F_2)_2$ also may be a polar complex with a dipole moment of 0.1 D or larger.[21]

(A) SCF Geometry Optimization. We examined various geometries of $(F_2)_2$ complexes employing, as a first approximation, the SCF scheme. The F–F distance of the fluorine molecule was taken to be 1.435 Å[29] in this section and kept unchanged throughout the complex calculation. Geometries of $(F_2)_2$ studied are schematically shown in Figure 5. In all the models the four atoms are assumed to be coplanar (C_s symmetry) and F_b, F_c, and F_d are collinear. Models I, III, and II have F_cF_d perpendicular to the F_aF_b axis at the midpoint of the F_aF_b bond, on the atom F_b, and at the midpoint of I and III, respectively. The intermolecular distance R is defined as the distance between F_c and the F_aF_b axis. All other models have F_cF_d rotated sequentially by 15° along the circular arc of which F_b is the center, with R being the F_b–F_c distance. Figure 6

Table XVII. Gross Atomic Electron Population of Isolated Molecules and Its Component Changes for the Complexes FCl-FH and ClF-HF[a,b]

	FCl		FH		$FCl \overset{(+)}{\underset{(-)}{\rightleftarrows}} FH$
	F_a	Cl	F_b	H	
Isolated molecules	9.3950	16.6050	9.4786	0.5214	
Total change	0.0274	−0.0165	0.0019	−0.0128	−0.0109
EX	0.0009	−0.0009	−0.0003	0.0003	
PL	0.0199	−0.0199	0.0127	−0.0127	
CT	0.0004	0.0108	−0.0101	−0.0011	−0.0112
MIX	0.0066	−0.0063	−0.0004	0.0007	0.0003
	ClF		HF		$ClF \overset{(+)}{\underset{(-)}{\rightleftarrows}} HF$
	Cl	F_a	H	F_b	
Isolated molecules	16.6050	9.3950	0.5214	9.4786	
Total change	−0.0538	0.0344	−0.0175	0.0369	0.0194
EX	0.0005	−0.0005	−0.0032	0.0032	
PL	−0.0508	0.0508	−0.0128	0.0128	
CT	−0.0035	−0.0147	0.0217	−0.0035	0.0182
MIX	−0.0001	−0.0011	−0.0231	0.0243	0.0012

[a] At the calculated equilibrium geometries. FCl-FH: r(Cl-F) = 2.737 Å, ∠ClFH = 141° and collinear FClF. ClF-HF: r(F-H) = 1.864 Å, ∠ClFH = 143° and collinear FHF. [b] For sign conventions, see Table II.

Table XVIII. The Dipole Moment Change $\Delta\mu$ and Its Components in D for the Anti-Hydrogen Bonded Complex FCl-FH at Experimental Geometry[a]

	μ_x[b]	μ_z[c]	$\lvert\mu\rvert$
Monomers[d]	2.07	2.55	3.28
$\Delta\mu$[e]	0.02	0.38	0.32
$\Delta\mu_{EX}$	−0.00	0.02	0.01
$\Delta\mu_{PL}$	0.02	0.20	0.17
$\Delta\mu_{CT}$	0.00	0.11	0.08
$\Delta\mu_{MIX}$	−0.00	0.05	0.04

[a] r(Cl-F_b) = 2.774 Å and ∠ClF_bH = 115°. γ = 0 is assumed in **10**. [b] Perpendicular to the F_aClF_b axis. A positive value corresponds to the polarity $^+H(F_aClF_b)^-$. [c] Parallel to the F_aClF_b axis. A positive value corresponds to the polarity $^-F_aClF_bH^+$. [d] The vector sum of the calculated monomer dipoles. [e] The total change of dipole moment upon complex formation: $\Delta\mu$ = μ(complex) − μ(monomers).

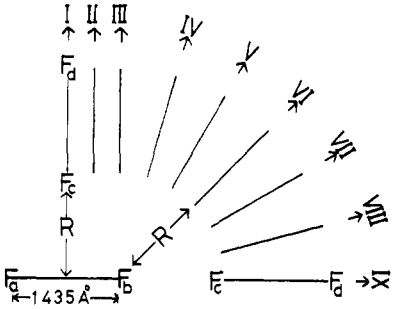

Figure 5. Assumed models I-IX for $(F_2)_2$. All atoms are in a plane. In models I-II, F_cF_d is perpendicular to F_aF_b with R being the distance between F_c and the bond F_aF_b. In models III to IX, F_b, F_c, and F_d are collinear with R being the F_bF_c distance.

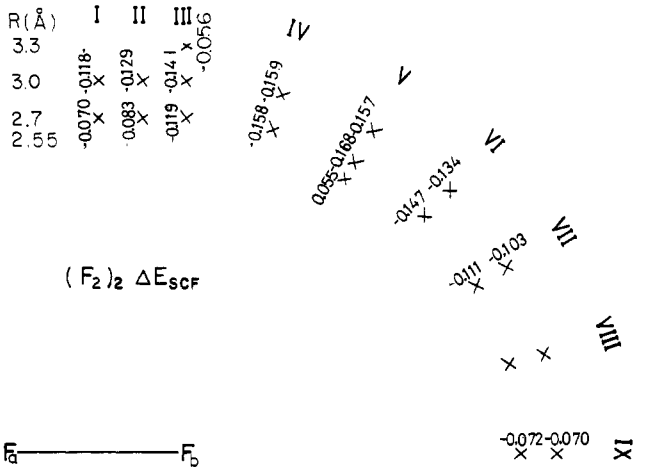

Figure 6. The SCF interaction energy ΔE_{SCF} for models in Figure 5. Two R's are 2.7 and 3.0 Å, respectively, where X's indicate the positions of the F_c atom. Exceptions are a point at R = 2.55 Å for V and another at R = 3.3 Å for III. The energies are in kcal/mol.

shows ΔE_{SCF} for R = 2.7 and 3.0 Å. The smaller R is chosen as a sum of the van der Waals radius (1.35 Å) of the F atoms.[37] A calculation at a smaller R = 2.55 Å for model V indicates that the complex is repulsive, suggesting that R = 2.7 Å can be taken as the most stable geometry. Another calculation at R = 3.3 Å for model III indicates that R = 3.0 Å is the best distance for this model. Additional calculations (not shown) were also carried out for several structures in which F_d is moved out of the plane of the complex (non-planar models) or F_d is kept within the plane but is made nonlinear with respect to the F_bF_c axis (nonlinear models). In all cases the complex formed is much less stable than the corresponding coplanar, collinear models. We may conclude, therefore, that the most stable geometry within ΔE_{SCF} is an open L-shaped structure, model V with R = 2.7 Å. The stability of the complex due to ΔE_{SCF} is extremely small.

(B) Dispersion Energy. Since the contribution of ΔE_{SCF} is so small, the dispersion energy DISP may be equally as important as the ΔE_{SCF} contribution. DISP, estimated by a second-order perturbation method, is shown in Figure 7. The DISP stabilization increases as the angle between the two fluorine molecules increases, reaching a maximum when F_aF_b and F_cF_d are collinear. This trend seems to be reasonable as will be discussed shortly. Though the contribution of DISP increases as R becomes smaller, the steep repulsion due to ΔE_{SCF} seems to keep the equilibrium R around 2.7 Å, as is seen for model V. Since the criteria of reliability of DISP

Table XIX. Energy Components (kcal/mol), Dipole Moment (D), and Atomic Population Change of the $(F_2)_2$ Complex for Various Models at R = 2.7 Å

	Model[a]				
	I	III	V	VII	IX
		Energy			
ΔE	−0.20	−0.23	−0.38	−0.42	−0.43
DISP	−0.13	−0.11	−0.21	−0.31	−0.36
ΔE_{SCF}	−0.07	−0.12	−0.17	−0.11	−0.07
ES	0.01	−0.06	−0.08	0.03	0.09
EX	0.39	0.38	0.33	0.26	0.23
PL	−0.00	−0.00	−0.00	−0.00	−0.00
CT	−0.46	−0.46	−0.42	−0.43	−0.38
MIX		0.03		0.03	
		Dipole Moment			
μ_{SCF}	0.021	0.033	0.040	0.018	0
μ_{PL}	0.000	0.014	0.021	0.013	0
$\mu_{CT+EX+MIX}$	0.021	0.019	0.019	0.005	0
		Atomic Population Change[b]			
F_a	−0.0005	−0.0023	−0.0027	−0.0024	−0.0023
F_b	−0.0005	0.0010	0.0015	0.0020	0.0023
F_c	0.0001	−0.0006	−0.0007	0.0011	0.0023
F_d	0.0009	0.0018	0.0018	−0.0007	−0.0023

[a] As defined in Figure 5. [b] Positive and negative values indicate an increase and a decrease, respectively, of electron population upon complex formation.

calculated in the present procedure are not as well established as those of ΔE_{SCF}, its absolute magnitude should not be taken too seriously. Due to the importance of DISP the total stabilization ΔE calculated as a simple sum ΔE_{SCF} + DISP, Table XIX, yields a linear equilibrium structure. A more quantitative balance in reliability between ΔE_{SCF} and DISP is required to make a sensible prediction of geometry.

DISP's preference for the linear geometry can be explained by examining the leading term in the perturbation sum, eq 3. While the numerator depends strongly on the mutual orientation as well as the distance R between the two monomers, the denominator in the present perturbation method is constant regardless of the geometry. A discriminatively large contribution for the linear geometry comes from the $\langle 7_A 10_A | 7_B 10_B \rangle$ integral, i.e., the interaction between the 7 → 10 transitions of the monomers, where the seventh MO is an occupied σ_g MO and the tenth MO is the lowest vacant σ_u* MO. This transition, whose moment is parallel to the F_2 molecular axis, yields the largest contribution to DISP when the two monomers are collinear. Since the numerator of eq 3 is the square of $\langle i_A - j_A | k_B l_B \rangle$, the term gives a $\cos^2\theta$-like angular dependence where $\theta = \angle F_a F_b F_c$.

(C) Energy Decomposition Analysis. The energy decomposition analysis of ΔE_{SCF} is also given in Table XIX. ES is merely a small contributor to the stabilization, though its angular dependency is the most pronounced. The magnitude of ES in Table XIX is consistent with an order-of-magnitude estimate based on the quadrupole-quadrupole interaction $E_{\theta\theta}$; by assuming the quadrupole moment of $F_2 = 1 \times 10^{-26}$ esu cm^2, $R = 2.7 + 0.5 = 3.2$ Å, one obtains $E_{\theta\theta}$ ca. −0.1 kcal/mol. The angular dependence, however, is different from what is expected from a consideration of only $E_{\theta\theta}$, which favors the "T" shape, model I. A tempting interpretation of ES as well as EX is based on the electron distribution of F_2, which is more dense (or more negative) to the direction of the π orbitals than the σ orbitals (the molecular axis). The linear model IX, which has a σ–σ or positive-positive contact of electron clouds, is very favorable for EX but is unfavorable for ES. In perpendicular models I and III there are two factors: an F_cF_b positive σ–F_aF_b negative π contact which has a favorable ES and an F_cF_d negative π–F_aF_b negative π contact which is undesirable for both ES and EX. A balance of these factors apparently favors the open L geometry of model V.

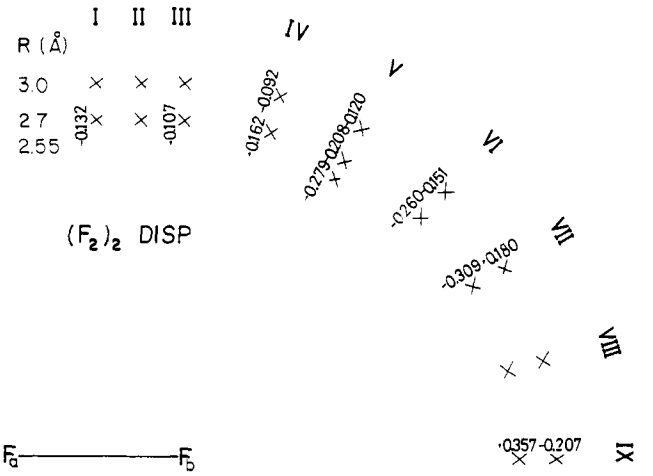

Figure 7. The dispersion energy DISP for models in Figure 5. For other details see Figure 6.

The absolute value of CT is rather small yet is the largest component for $(F_2)_2$. Surprisingly its magnitude depends only weakly on the angle. For the T-shaped model I $\pi \rightarrow \sigma^*$ and $\pi \rightarrow \pi^*$ type overlap are the dominant contributions to CT.

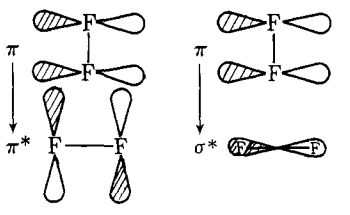

For the linear model IX, another type of overlap, $\sigma \rightarrow \sigma^*$, is the dominant contribution.

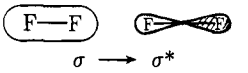

Table XX. Energy Components (kcal/mol) at the Optimized Intermolecular Separation R_e and Qualitative Classification of EDA Complexes with the 4-31G Basis Set

Donor–Acceptor	Type	R_e, Å	ΔE_{SCF}	ES	EX	PL	CT	MIX	Classification[a]
H_3N-BF_3[b]	n–σ^*	1.60	−71.5	−142.3	136.3	−42.7	−52.7	29.9	Strong ES
H_3N-BH_3[b]	n–σ^*	1.70	−44.7	−92.9	86.9	−17.2	−27.1	5.6	Strong ES
$OC-BH_3$[b]	$\sigma-\sigma^*$	1.63	−28.5	−60.9	98.9	−61.8	−68.3	63.6	Strong CT–PL–ES
	$\pi^*-\pi$								
H_3N-ClF	n–σ^*	2.72	−8.2	−11.2	7.4	−1.1	−3.6	0.2	Intermediate ES
$H_2O-OC(CN)_2$[c]	n–π^*	2.70	−8.0	−9.7	4.4	−1.0	−1.8[d]		Intermediate ES
$HF-ClF$	n–σ^*	2.74	−3.4	−3.6	1.8	−0.2	−1.4	0.1	Weak ES
H_3N-Cl_2	n–σ^*	2.93[e]	−2.9	−4.0	3.9	−0.8	−2.3	0.3	Weak ES–CT
Benzene–$OC(CN)_2$[f,g]	$\pi-\pi^*$	3.6–3.8							Weak ES–DISP
H_3N-F_2	n–σ^*	3.00	−1.1	−0.8	0.6	−0.3	−0.6	0.0	Weak ES–CT
H_2CO-F_2	n–σ^*	2.91	−0.7	−0.4	0.3	−0.1	−0.5	0.0	Weak CT–ES–DISP
$H_2CO-C_2H_4$[f]	$\pi-\pi$	3.75	−0.7	−0.5	0.4	−0.1	−0.5[d]		Weak CT–ES
F_2-F_2	$\pi-\sigma^*$	2.7	−0.2	−0.1	0.3	0.0	−0.4	0.0	Weak DISP–CT

[a] Qualitative classification based on the predominant contributions which are 50% or more of the largest contribution. See text. [b] Reference 14. [c] Reference 12. [d] CT + MIX. [e] Not optimized. [f] Reference 13. [g] Only STO-3G calculations have been carried out.

Apparently the contributions are of comparable magnitude, giving rise to a small overall CT angular dependence.

(D) Dipole Moment. As a measure of the polarity of this complex, the dipole moment μ should be examined. The SCF dipole moment and its components are shown in Table XIX. It is interesting to note that the model V of maximum dipole moment coincides with that of the best ΔE_{SCF}. Components of the dipole moment and atomic population changes due to complex formation, also shown in Table XIX, suggest a rather complicated motion of electrons (mainly due to PL and CT) is taking place as the geometry changes from I through III to IX. The contribution of the dispersion interaction to the dipole moment is calculated from the first-order dispersion-perturbed wave function ψ.

$$\psi = A_0B_0 - \sum_i^{occ}\sum_k^{vac}\sum_\mu^{occ}\sum_\nu^{vac}\frac{\langle A_0B_0|H'|A_{i\to k}B_{\mu\to\nu}\rangle}{E_{i_A\to k_A,\mu_B\to\nu_B} - E_0} \times A_{i\to k}B_{\mu\to\nu} \quad (4)$$

where A_0B_0 is the Hartree product of the Hartree–Fock wave functions of the ground state of the molecule A and B, $A_{i\to k}B_{\mu\to\nu}$ is the Hartree product of the wave functions for the singly excited states of A and B.[13] The calculated dispersion contribution to the dipole moment is found to be negligible (<0.001 D).

The largest calculated dipole moment $\mu_{SCF} \sim 0.04$ D (model V) is substantially smaller than the experimental estimate (>0.1 D). The origin of this discrepancy is not obvious. It is possible, though unlikely, that the calculated R_e is too large; if R_e is smaller than 2.7 Å by 0.2–0.3 Å, the calculated μ_{SCF} becomes comparable to the experimental threshold and the optimum geometry by ΔE_{SCF} + DISP would be similar to model V. It may also be dependent on the basis set or influenced by the correlation effect.[38] We did not test either of these conjectures.

VII. Discussion and Conclusions

Energy decomposition results employing the 4-31G basis set at calculated equilibrium geometries of each of the EDA complexes examined in this paper as well as in the previous papers of our series are summarized in Table XX. Very qualitative classifications have also been given. In those cases in which truncated potential energy calculations have been carried out, the classification is based on what components are required to maintain the binding characteristics of the complex. When this has not been done, those contributions whose magnitude was greater than 50% of that of the largest component were assumed to be essential to the binding. Since 4-31G set exaggerates the ES contribution, the corresponding percentage for a calculation with a larger basis set would be about 70%. Anyway, the classifications are meant to be only a qualitative guide to the nature of complex binding and should not be taken as an absolute, definitive categorization. For instance HF–ClF and H_3N–ClF have been tentatively labeled as "ES complexes" in Table XX, one may equally as well call them "ES–CT", or still better "ES > CT complexes".

In Table XX, certain trends in the origin of stabilization among varieties of EDA complexes are evident. Three classes are recognized for n–σ^* type complexes. A polar–polar complex is the strongest and is dominated by a large ES contribution even though CT and PL are not negligible. $OC-BH_3$ is an exceptional, strong CT–PL–ES complex, which arises from CO's duality in the CT interaction, acting both as a σ donor and a π^* acceptor. A polar–nonpolar complex is intermediate to weak, with both ES and CT being major contributions. A nonpolar–nonpolar complex is very weak, with both DISP and CT contributing to the stabilization. A polar n donor–π^* acceptor complex seems to be a weak to intermediate ES complex, whereas a π donor–π^* acceptor looks to be of ES–DISP type. Further detailed elaboration of the classification of EDA complexes will be deferred to subsequent papers.

For H_3N– and H_2CO–halogen complexes studied in the paper, the following conclusions can be made in addition to those included in Table XX.

(i) A deviation of H_3N–halogen complexes from the C_{3v} geometry results in destabilization due to ES and EX, which may be explained in terms of difference in electron distribution of the halogens in the π and σ directions.

(ii) All the components of the Cl_2 complex are larger than the corresponding components for the F_2 complex. This may be interpreted as the result of the difference in the size of electron distribution.

(iii) The *N*-methyl substituent effect is small due to a cancellation of the EX and CT components. This is compared with a small substituent effect for H_3N-BH_3, which is the result of PL–EX cancellation, and a large effect for H_3N-H^+, which is due to PL.

For FCl–FH anti-hydrogen bonded and ClF–HF hydrogen bonded complexes, the following additional conclusions can be drawn.

(i) The energies of the two forms appear to be very similar: the 4-31G set prefers ClF–HF, while the larger 4-31G** set favors FCl–FH.

(ii) The calculated geometry of FCl–FH is in good agreement with experiment.

(iii) The geometry of ClF–HF is predicted to be: r(F–F) ~ 2.86 Å, ∠ClF–H ~ 130°, and ∠FHF ~ 180°.

(iv) The deviation of F_a from the collinearity in F_aCl-F_bH is not favorable due to EX, supplemented by ES or CT de-

pending on the mode of deviation. This may be explained in terms of differences in the electron distribution in ClF between π and σ directions.

(v) The major difference in the energy components between FCl–FH and ClF–HF is EX.

For $(F_2)_2$ the additional conclusions are:

(i) ΔE_{SCF} favors an "open L" shape structure with an angle of 120°, the shortest intermolecular F–F separation being 2.7 Å. This shape is a result of different competing overlaps between occupied and vacant MO's.

(ii) DISP prefers a linear structure, which gives a favorable alignment of σ–σ^* transition dipoles.

(iii) CT is the largest source of ΔE_{SCF}, whose angular dependence is controlled by a balance of different modes of MO overlaps.

(iv) The calculated dipole moment is ~0.04 D, smaller than the experimental estimate.

Acknowledgments. The authors are grateful to Drs. R. S. Mulliken, A. D. Buckingham, J. S. Muenter, J. S. Winn, S. E. Novick, and K. Kitaura for stimulating discussions and to J. O. Noell for a critical reading of the manuscript. The research is in part supported by the National Science Foundation and the Public Health Research Grant No. CA-14170 from the National Cancer Institute. H.U. is on leave from Kitasato University, Tokyo, Japan.

References and Notes

(1) (a) G. C. Pimentel and A. L. McClellan, "The Hydrogen Bond", W. H. Freeman, San Francisco, Calif., 1960; (b) M. D. Joesten and L. J. Schaad, "Hydrogen Bonding", Marcel Dekker, New York, N.Y., 1974.
(2) (a) G. Briegleb, "Electronen-Donor-Acceptor-Komplexes", Springer-Verlag, West Berlin, 1961; (b) L. J. Andrews and R. M. Keefer, "Molecular Complexes in Organic Chemistry", Holden-Day, San Francisco, Calif., 1964; (c) J. Rose, "Molecular Complexes", Pergamon Press, Oxford, 1967; (d) R. Foster, "Organic Charge Transfer Complexes", Academic Press, New York, N.Y., 1969, (e) J. Yarwood, "Spectroscopy and Structure of Molecular Complexes", Plenum Press, London, 1973.
(3) R. S. Mulliken, *J. Am. Chem. Soc.*, **72**, 600 (1950).
(4) M. W. Hanna, *J. Am. Chem. Soc.*, **90**, 285 (1968); J. L. Lippert, M. W. Hanna, and P. J. Trotter, *ibid.*, **91**, 4035 (1969). See also R. J. W. Le Fèvre, D. V. Radford, and P. J. Stiles, *J. Chem. Soc. B*, 1297 (1968).
(5) R. S. Mulliken and W. B. Person, *J. Am. Chem. Soc.*, **91**, 3409 (1969).
(6) (a) K. Morokuma and L. Pedersen, *J. Chem. Phys.*, **48**, 3275 (1968); (b) Recent reviews, P. A. Kollman and L. C. Allen, *Chem. Rev.*, **72**, 283 (1972), and P. A. Kollman, to be published in "Modern Theoretical Chemistry", H. F. Schaefer, Ed., Plenum Press, New York, N.Y., 1976.
(7) K. Morokuma, *J. Chem. Phys.*, **55**, 1236 (1971).
(8) K. Kitaura and K. Morokuma, *Int. J. Quantum Chem.*, **10**, 325 (1976).
(9) S. Iwata and K. Morokuma, *J. Am. Chem. Soc.*, **95**, 7563 (1973); **97**, 955 (1975).
(10) S. Yamabe and K. Morokuma, *J. Am. Chem. Soc.*, **97**, 4458 (1975).
(11) K. Morokuma, S. Iwata, and W. A. Lathan, "The World of Quantum Chemistry", R. Daudel and B. Pullman, Ed., D. Reidel Publishing Co., Dordrecht, Holland, 1974, p 277.
(12) Part 1: W. A. Lathan and K. Morokuma, *J. Am. Chem. Soc.*, **97**, 3615 (1975).
(13) Part 2: W. A. Lathan, G. R. Pack, and K. Morokuma, *J. Am. Chem. Soc.*, **97**, 6624 (1975).
(14) Part 3: H. Umeyama and K. Morokuma, *J. Am. Chem. Soc.*, **98**, 7208 (1976).
(15) H. Umeyama and K. Morokuma, *J. Am. Chem. Soc.*, **98**, 4400 (1976).
(16) (a) H. Margenau, *Rev. Mod. Phys.*, 11, 1 (1939); (b) H. Margenau and N. R. Kestner, "Theory of Intermolecular Forces", 2nd ed, Pergamon Press, New York, N.Y., 1971: (c) J. O. Hirschfelder, C. F. Curtis, and R. B. Bird, "Theory of Gases and Liquids", Wiley, New York, N.Y., 1964.
(17) In papers 1 and 2 of the series[12,13] the old method of Morokuma[7] has been used with lower case symbols es, pl, ex, and ct. In paper 3[14] and the present paper, the new method of Kitaura and Morokuma[8] is used with upper case symbols ES, PL, EX, CT, and MIX. The new components are equal to the old corresponding components, ES = es, PL = pl, and EX = ex, except that CT + MIX = ct. The new method allows the old "charge transfer" term ct to be decomposed further into the true charge transfer term and the coupling term. In 3 and the present paper, a negative (positive) value corresponds to a stabilization (destabilization), while in 1 and 2 an opposite convention is used.
(18) R. R. Lucchese and H. F. Schaefer, *J. Am. Chem. Soc.*, **97**, 7205 (1975).
(19) K. C. Janda, W. Klemperer, and S. E. Novick, *J. Chem. Phys.*, **64**, 2698 (1976).
(20) S. J. Harris, S. E. Novick, J. S. Winn, and W. Klemperer, *J. Chem. Phys.*, **61**, 3866 (1974).
(21) Private communication from W. Klemperer and J. S. Winn.
(22) (a) R. Ditchfield, W. J. Hehre, and J. A. Pople, *J. Chem. Phys.*, **51**, 2657 (1969); (b) W. J. Hehre, W. A. Lathan, R. Ditchfield, M. D. Newton, and J. A. Pople, Quantum Chemistry Program Exchange, Indiana University, 1973.
(23) H. Umeyama and K. Morokuma, *J. Am. Chem. Soc.*, in press.
(24) P. C. Hariharan and J. A. Pople, *Theor. Chin. Acta*, **28**, 213 (1973).
(25) E. Clementi, J. Mehl, and H. Popkie, IBMOL5A, unpublished. Acknowledgement is made to Drs. M. van Hemert and E. Clementi for making the IBMOLH program available.
(26) B. Rosen, "Spectroscopic Data Relative to Diatomic Molecules", Pergamon Press, Oxford, 1970.
(27) G. Herzberg, "Electronic Spectra of Polyatomic Molecules", Van Nostrand, New York, N.Y., 1966.
(28) J. E. Wollrab and V. M. Laurie, *J. Chem. Phys.*, **51**, 1580 (1969).
(29) G. Herzberg, "Spectra of Diatomic Molecules", Van Nostrand, New York, N.Y., 1950.
(30) S. Green, *J. Chem. Phys.*, **58**, 3117 (1973); S. Green, *Adv. Chem. Phys.*, **25**, 179 (1974).
(31) S. Nagakura, *J. Am. Chem. Soc.*, **80**, 520 (1958).
(32) (a) D. H. Aue, H. M. Webb, and M. T. Bowers, *J. Am. Chem. Soc.*, **94**, 4726 (1972); M. T. Bowers, D. H. Aue, H. M. Webb, and R. T. McIver, *ibid.*, **93**, 4313 (1971); (b) W. G. Henderson, J. L. Beauchamp, D. Holtz, and R. W. Taft, *ibid.*, **94**, 4724 (1972); (c) E. M. Arnett, *Acc. Chem. Res.*, **6**, 404 (1973); (d) J. L. Beauchamp, *Annu. Rev. Phys. Chem.*, **22**, 527 (1971).
(33) R. F. McCoy and S. H. Bauer, *J. Am. Chem. Soc.*, **78**, 2061 (1956).
(34) K. Watanabe, T. Nakamura, and J. R. Mottl, *J. Quant. Spectrosc. Radiat. Transfer*, **2**, 369 (1962).
(35) O. Hassel and K. O. Stroemme, *Acta Chem. Scand.*, **13**, 275 (1959).
(36) T. R. Dyke, B. J. Howard, and W. Klemperer, *J. Chem. Phys.*, **56**, 2442 (1972).
(37) L. Pauling, "The Nature of the Chemical Bond", 3rd ed, Cornell University Press, Ithaca, N.Y., 1960.
(38) G. Das and A. C. Wahl, *J. Chem. Phys.*, **56**, 3532 (1972).